Single-loop system reliability-based topology optimization considering statistical dependence between limit-states

Tam H. Nguyen · Junho Song · Glaucio H. Paulino

Abstract This paper presents a single-loop algorithm for system reliability-based topology optimization (SRBTO) that can account for statistical dependence between multiple limit-states, and its applications to computationally demanding topology optimization (TO) problems. A single-loop reliability-based design optimization (RBDO) algorithm replaces the inner-loop iterations to evaluate probabilistic constraints by a non-iterative approximation. The proposed single-loop SRBTO algorithm accounts for the statistical dependence between the limit-states by using the matrix-based system reliability (MSR) method to compute the system failure probability and its parameter sensitivities. The SRBTO/MSR approach is applicable to general system events including series, parallel, cut-set and link-set systems and provides the gradients of the system failure probability to facilitate gradient-based optimization. In most RBTO applications, probabilistic constraints are evaluated by use of the first-order reliability method for efficiency. In order to improve the accuracy of the reliability calculations for RBDO or RBTO problems with high nonlinearity, we introduce a new single-loop RBDO scheme utilizing the second-order reliability method and implement it to the proposed SRBTO algorithm. Moreover, in order to overcome challenges in applying the proposed algorithm to computationally demanding topology optimization problems, we utilize the multiresolution topology optimization (MTOP)

T. H. Nguyen · J. Song · G. H. Paulino (✉)
Dept. of Civil and Environmental Engineering,
Univ. of Illinois, Urbana, IL 61801, USA
e-mail: paulino@illinois.edu

T. H. Nguyen
e-mail: tnguyen3@illinois.edu

J. Song
e-mail: junho@illinois.edu

method, which achieves computational efficiency in topology optimization by assigning different levels of resolutions to three meshes representing finite element analysis, design variables and material density distribution respectively. The paper provides numerical examples of two- and three-dimensional topology optimization problems to demonstrate the proposed SRBTO algorithm and its applications. The optimal topologies from deterministic, component and system RBTOs are compared with one another to investigate the impact of optimization schemes on final topologies. Monte Carlo simulations are also performed to verify the accuracy of the failure probabilities computed by the proposed approach.

1 Introduction

Topology optimization aims to find an optimal structural layout under given constraints through iterative computational simulations. In the past decades, a large number of studies have been devoted to this important research area of structural optimization (Bendsøe and Sigmund 2003). Topology optimization methods have been successfully applied to a wide range of practical engineering problems (Rozvany 2001; Bendsøe and Sigmund 2003). However, most of the efforts have been conducted in a deterministic manner although uncertainties in loads or material properties may result in significant likelihood of violating design constraints. In the current study, this approach is referred to as deterministic topology optimization (DTO). Recently,

active research has been performed to achieve optimal topologies with acceptable probability of satisfying given constraints. This approach is often termed as reliability-based topology optimization (RBTO), and has been successfully applied to a variety of topology optimization problems (Bae et al. 2002; Maute and Frangopol 2003; Allen et al. 2004; Jung and Cho 2004; Kang et al. 2004; Kharmanda et al. 2004; Kim et al. 2006; Guest and Igusa 2008; Rozvany 2008; Lógó et al. 2009; Luo et al. 2009; Chen et al. 2010). For example, Maute and Frangopol (2003) employed RBTO in the design of compliant micro-electromechanical system mechanism (MEMS). Jung and Cho (2004) applied RBTO to geometrically nonlinear structures with uncertain loads and material properties. Additionally, Rozvany (2008) derived the analytical solution for benchmark problems in probabilistic topology optimization. Most research efforts on RBTO have been focused on satisfying the probabilistic constraint given for each failure mode. In this paper, this approach is referred to as *component* reliability-based topology optimization (CRBTO). A generic formulation for CRBTO problems is given as follows

$$
\min_{\mathbf{d}} f(\rho(\boldsymbol{\psi}; \mathbf{d}))
$$
$$
s.t. \ P[g_i(\rho(\boldsymbol{\psi}; \mathbf{d}), \mathbf{X}) \le 0] \le P_i^t, \quad i = 1, ..., n
$$
$$
\mathbf{K}(\rho(\boldsymbol{\psi}; \mathbf{d})) \cdot \mathbf{u}_d = \mathbf{f}
$$
$$
\mathbf{d}^L \le \mathbf{d} \le \mathbf{d}^U
$$

$$(1)$$

where $\mathbf{d} \in \Re^k$ is the vector of deterministic design variables; $\rho(\boldsymbol{\psi}; \mathbf{d})$ is the material density at the position $\boldsymbol{\psi} \in \Re^2$ or $\Re^3$ that is generally determined by a projection function $f_p(\cdot)$ and the design variables, i.e. $\rho(\boldsymbol{\psi}; \mathbf{d}) = f_p(\mathbf{d})$; $f(\cdot)$ is the objective function that often describes the volume, compliance, or displacement of the structure; $\mathbf{X} \in \Re^m$ is the vector of random variables representing the uncertainties in the problem; $g_i(\cdot)$, $i = 1, \dots, n$ is the i-th "limit-state function" that indicates violating a design constraint given in terms of volume, displacement, or compliance by its negative sign, i.e. $g_i(\cdot) \le 0$; P_i^t is the constraint on the probability of the i-th limit state; $\mathbf{K}$, $\mathbf{u}_d$ and $\mathbf{f}$ respectively denote the stiffness matrix, displacement vector and load vector in the equilibrium condition; and $\mathbf{d}^L$ and $\mathbf{d}^U$ are the lower and upper bounds on $\mathbf{d}$, respectively. For simplicity, the equilibrium condition and the bounds on the design variables will be omitted in the following RBTO formulations of the paper. The probability constraint in (1) is described in terms of either the reliability index (RIA: Enevoldsen and Sørensen 1994) or the performance function, i.e. the P_i^t-quantile of the limit-state function (PMA: Tu et al. 1999), which is obtained by use of a structural reliability analysis method such as the first-order reliability method (FORM).

While most research efforts in the literature have been focused on CRBTO, in certain circumstances, the prob- abilistic constraint should be given on a *system* failure event, i.e. a logical (or Boolean) function of multiple failure modes. For example, the failure of a topology design can be defined as an event that at least one of the potential failure modes occurs. This is termed as *system* reliability-based topology optimization (SRBTO). SRBTO introduces additional complexity to reliability calculations especially when component events are statistically dependent, or when the system event is not a series (i.e. union of events) or parallel system (i.e. intersection of events). A generic formulation for SRBTO is as follows.

$$
\min_{\mathbf{d}} f(\rho(\boldsymbol{\psi}; \mathbf{d}))
$$
$$
s.t. \ P(E_{sys}) = P\left[\bigcup_k \bigcap_{i \in C_k} g_i(\rho(\boldsymbol{\psi}; \mathbf{d}), \mathbf{X}) \le 0 \right] \le P_{sys}^t,
$$

$$(2)$$

where $P(E_{sys})$ is the probability of the system failure event; C_k is the index set of the components (limit-states) in the k-th cut-set; and P_{sys}^t is the constraint on the system failure probability. Any type of system event may be considered in SRBTO but, for illustration purpose, (2) shows a cut-set system formulation that can describe series, parallel, and cut-set systems. A limited number of studies have been performed on SRBTO because calculation of system probability and its parameter sensitivities introduces additional complexity to the topology optimization that already requires high computational cost. Recently, SRBTO has been considered for cases in which all component events are statistically independent of each other (Silva et al. 2010). In this case, the system failure probability and its parameter sensitivities can be obtained by algebraic calculations of the component probabilities and sensitivities. However, the limit-states of SRBTO problems often show strong statistical dependence because of shared or correlated random variables. In another recent research, SRBTO was applied to discrete structures that usually require less computational cost than continuum topology optimization (Mogami et al. 2006). However, the discrete approach (or so-called size approach) cannot change the structural topology during the solution process, so the solution will have the same topology as the initial design (Eschenauer and Olhoff 2001) whereas continuum topology optimization can optimize size, shape and connectivity of the structure.

As an effort to overcome impediments to adopting SRBTO techniques in current design practice, this study focuses on developing new SRBTO algorithms for continuum linear elastic structures that can consider statistical dependence between component events (limit-states). First, we introduce an SRBTO procedure using a matrix-based system reliability (MSR) method (Song and Kang 2009; Kang et al. 2011) to handle the statistical depen-

dence between the limit-states. The MSR method allows for accurate and efficient calculation of system failure probability and its parameter sensitivities for general system problems including series, parallel, cut-set and link-set systems. Second, we develop a new single-loop algorithm to improve the accuracy of FORM-based RBTO by use of the second-order reliability method (SORM). Finally, a recently developed multiresolution topology optimization (MTOP; Nguyen 2010; Nguyen et al. 2010a) is integrated with the SRBTO algorithm to enhance efficiency in computationally demanding topology optimization problems. This approach uses three distinct meshes with different resolutions for finite elements, density and design variables in order to achieve high resolution optimal designs with significantly reduced computational costs.

The remaining of this paper is structured as follows: Section 2 describes the single-loop system reliability-based topology optimization using the matrix-based system reliability method; Section 3 provides a single-loop algorithm to enhance component and system reliability-based topology optimization by use of the second-order reliability method; Section 4 presents the multiresolution topology optimization approach; Section 5 provides numerical examples of SRBTO; and finally Section 6 provides summary and conclusions of the paper.

2 System reliability-based topology optimization using matrix-based system reliability method

In this section, we present a single-loop formulation for system reliability-based topology optimization that can account for statistical dependence between limit-states for general system failure events. After a brief review on existing single-loop approaches for component and system RBTO and methods to account for statistical dependence, the new SRBTO formulation using matrix-based system reliability (MSR) method is introduced.

2.1 Single-loop component and system reliability-based topology optimization

For CRBTO and SRBTO shown in (1) and (2) respectively, a nested or "double-loop" approach has been often used, in which each step of the iterations for design optimization involves another loop of iterations for reliability analysis. However, this double-loop computation can be prohibitive if the computational cost for evaluating limit-state function(s) during the inner-loop search for the "most probable point" (MPP) or "design point" is expensive (Yang et al. 2005). There have been active research efforts to overcome this computational challenge by decoupling the reliability analysis and the design optimization loops (Wu and Wang 1998;

Royset et al. 2001; Du and Chen 2004; Liang et al. 2007, 2008; Shan and Wang 2008). For example, a single-loop approach (Liang et al. 2007, 2008) replaces the inner-loop calculations by an approximate solution obtained by the Karush–Kuhn–Tucker (KKT) optimality condition. As a result, the double-loop optimization problem is converted into an equivalent single-loop problem. This single-loop approach was reported to have the accuracy comparable with the double-loop approach and the efficiency almost equivalent to that of deterministic optimization (Liang et al. 2008). In this study, we utilize this single-loop approach for the RBTO formulations.

For the CRBTO problem in (1), the single-loop formulation is given as follows.

$$\min_{\mathbf{d}} f(\rho(\boldsymbol{\psi}; \mathbf{d}))$$

$$s.t. \quad g_{P_i^t} \cong g_i\left(\rho(\boldsymbol{\psi}; \mathbf{d}), \mathbf{x}(\mathbf{u}_i^t)\right) \geq 0, i = 1, ..., n$$

$$\text{where} \quad \mathbf{u}_i^t \cong \beta_i^t \cdot (\hat{\boldsymbol{\alpha}}_i^t)^T$$

$$\hat{\boldsymbol{\alpha}}_i^t \cong \left(-\frac{\nabla_{\mathbf{x}} g_i(\rho(\boldsymbol{\psi}; \mathbf{d}), \mathbf{x}(\mathbf{u}))\mathbf{J}_{\mathbf{x},\mathbf{u}}}{\left\|\nabla_{\mathbf{x}} g_i(\rho(\boldsymbol{\psi}; \mathbf{d}), \mathbf{x}(\mathbf{u}))\mathbf{J}_{\mathbf{x},\mathbf{u}}\right\|}\right)_{\mathbf{u}=\tilde{\mathbf{u}}_i} \quad (3)$$

where $g_{P_i^t}$ is the P_i^t-quantile of the i-th limit-state function $g_i(\cdot)$; $\beta_i^t = -\Phi^{-1}(P_i^t)$ is the target (generalized) reliability index where $\Phi^{-1}(\cdot)$ denotes the inverse cumulative distribution function (CDF) of the standard normal distribution; $\mathbf{J}_{\mathbf{x},\mathbf{u}}$ is the Jacobian matrix of the transformation from the standard normal space to the original random variable space, i.e. $\mathbf{x} = \mathbf{x}(\mathbf{u})$; $\hat{\boldsymbol{\alpha}}_i^t$ is the negative normalized gradient (row) vector of the i-th limit-state function evaluated at the approximate location for the performance function value $\tilde{\mathbf{u}}_i$. Instead of searching for the exact MPP at each step of the design iterations, the single-loop approach obtains an approximate location for the performance function value $\tilde{\mathbf{u}}_i$ by solving the system equation given by the KKT condition (Liang et al. 2008). Then, the negative normalized gradient is scaled by the target reliability index β_i^t to determine the location where $g_{P_i^t}$ is approximately evaluated, i.e. $\mathbf{u}_i^t$.

Similarly, the SRBTO problem in (2) can be solved by a single-loop approach as follows.

$$\min_{\mathbf{d},\mathbf{P}^t} f(\rho(\boldsymbol{\psi}; \mathbf{d}))$$

$$s.t. \quad g_{P_i^t} \cong g_i\left(\rho(\boldsymbol{\psi}; \mathbf{d}), \mathbf{x}(\mathbf{u}_i^t)\right) \geq 0, i = 1, ..., n$$

$$P(E_{sys}; \mathbf{P}^t) = P\left[\bigcup_k \bigcap_{i \in C_k} g_i(\rho(\boldsymbol{\psi}; \mathbf{d}), \mathbf{X}) \leq 0\right] \leq P_{sys}^t$$

$$\text{where} \quad \mathbf{u}_i^t \cong \beta_i^t \cdot (\hat{\boldsymbol{\alpha}}_i^t)^T$$

$$\hat{\boldsymbol{\alpha}}_i^t \cong \left(-\frac{\nabla_{\mathbf{x}} g_i(\rho(\boldsymbol{\psi}; \mathbf{d}), \mathbf{x}(\mathbf{u}))\mathbf{J}_{\mathbf{x},\mathbf{u}}}{\left\|\nabla_{\mathbf{x}} g_i(\rho(\boldsymbol{\psi}; \mathbf{d}), \mathbf{x}(\mathbf{u}))\mathbf{J}_{\mathbf{x},\mathbf{u}}\right\|}\right)_{\mathbf{u}=\tilde{\mathbf{u}}_i} \quad (4)$$

where $\mathbf{P}^t$ is the vector of the target failure probabilities, $P_i^t, i = 1, \ldots, n$. Note that in (4), the target failure probabilities are treated as design variables rather than predefined constraint values as in (3). This is to control the system failure probability $P(E_{sys})$ indirectly in the single-loop approach by controlling the radii $\beta_i^t = -\Phi^{-1}(P_i^t)$, $i = 1, \ldots, n$ of the spheres on which the approximate location for the performance function values are found.

2.2 System reliability-based topology optimization under statistical dependence

When the limit-states in an SRBTO problem are assumed to be statistically independent (Silva et al. 2010), the system probability can be computed by algebraic calculations of the probabilities of the individual limit-states because the probability of any intersection can be computed by the product of the individual component probabilities. However, if there exists significant statistical dependence between limit-states due to shared or correlated random variables, one needs to use system reliability analysis methods that can account for the dependence. In addition, the parameter sensitivities of the system failure probability would facilitate the use of gradient-based optimization algorithm. However, computation of the parameter sensitivities of a system failure probability is challenging when component events are statistically dependent or the system event is not a series or parallel system.

The authors have recently applied the matrix-based system reliability (MSR) method to general reliability-based design optimization problems (Nguyen et al. 2010b). The current study aims to use the MSR method for SRBTO. The MSR method (Song and Kang 2009) computes the probability of a general system including series, parallel, cut-set and link-set system and its parameter sensitivities by systematic matrix calculations. Consider a system event whose i-th component, $i = 1, \ldots, n$ has two distinct states, e.g. failure or survival. Then, the sample space can be subdivided into $N = 2^n$ mutually exclusive and collectively exhaustive (MECE) events, denoted by $e_j, j = 1, .., N$. Then, any system event can be represented by an "event" vector $\mathbf{c}$ whose j-th element is 1 if e_j belongs to the system event and 0 otherwise. Let $p_j = P(e_j), j = 1, .., N$ denote the probability of e_j. Due to the e_j's mutual exclusiveness, the probability of any general system event E_{sys}, i.e. $P(E_{sys})$ is computed as the sum of the probabilities of e_j's that belong to the system event. Therefore, the system probability is computed by the inner product of the two vectors, that is

$$P(E_{sys}) = \begin{cases} \int_{\mathbf{s}} \mathbf{c}^T \mathbf{p}(\mathbf{s}) f_{\mathbf{S}}(\mathbf{s}) d\mathbf{s} & \text{dependent components} \\ \mathbf{c}^T \mathbf{p} & \text{independent components} \end{cases}$$
(5)

where $\mathbf{p}$ is the "probability" vector that contains p_j's, $j = 1, .., N$; $\mathbf{S}$ denotes the random variables identified as the sources of statistical dependence between components, termed as common source random variables (CSRVs). For a given outcome of CSRVs, the component events are conditionally independent of each other, which allows us to use the efficient procedure to construct the probability vector that is applicable to independent components (Song and Kang 2009); $\mathbf{p}(\mathbf{s})$ denotes the probability vector constructed by use of the conditional failure probabilities of the limit-states given $\mathbf{S} = \mathbf{s}$, i.e. $P_i(\mathbf{s}) \equiv P(E_i|\mathbf{S} = \mathbf{s})$ instead of $P_i \equiv P(E_i)$; and $f_{\mathbf{S}}(\mathbf{s})$ is joint probability density function (PDF) of $\mathbf{S}$. Matrix-based procedures have been developed to construct the vectors $\mathbf{c}$ and $\mathbf{p}$ efficiently; to compute conditional probabilities and component importance measures; and to evaluate parameter sensitivities of the system failure probability. The details of these procedures and merits of the method are summarized in (Song and Kang 2009). The method has been further developed and successfully applied to various system reliability problems (Kang et al. 2008, 2011; Song and Ok 2010; Lee et al. 2011).

When CSRVs are not clearly shown as in Kang et al. (2008), one can identify the source of statistical dependence between limit-states from the results of the component reliability analyses. For example, when the first-order reliability method (FORM) is used for the component reliability analyses, the component events are described as $Z_i \leq -\beta_i$, $i = 1, \ldots, n$, where Z_i and β_i respectively denote the standard normal random variable and the reliability index obtained by FORM. If $Z_i, i = 1, \ldots, n$, follow the generalized Dunnett–Sobel (DS) class correlation model (Dunnett and Sobel 1955; Song and Kang 2009), they are represented in the form:

$$Z_i = \left(1 - \sum_{k=1}^{m} r_{ik}^2\right)^{0.5} Y_i + \sum_{k=1}^{m} r_{ik} S_k, \quad i = 1, \ldots, n \quad (6)$$

in which $Y_i, i = 1, \ldots, n$ and $S_k, i = 1, \ldots, m$ are uncorrelated standard normal random variables; and r_{ik}'s are the coefficients of the generalized DS model that determine the correlation coefficient between Z_i and Z_j as $\rho_{ij} = \sum_{k=1}^{m} (r_{ik} . r_{jk})$ for $i \neq j$. Note Z_i and Z_j are conditionally independent of each other given the outcome of CSRVs $S_k, i = 1, \ldots, m$. Thus, the conditional probability of the i-th component event given $\mathbf{S} = \mathbf{s}$ is derived as

$$P_i(\mathbf{s}) = P(Z_i \leq -\beta_i|\mathbf{s}) = \Phi\left(\frac{-\beta_i - \Sigma_{k=1}^{m}(r_{ik}s_k)}{\sqrt{1 - \Sigma_{k=1}^{m} r_{ik}^2}}\right) \quad (7)$$

If a given correlation matrix cannot be described exactly by a generalized DS class, one can obtain a generalized DS

model with the minimum fitting error for an approximate identification of CSRVs (Kang et al. 2011).

2.3 Single-loop SRBTO algorithm using MSR method

The single-loop SRBTO using the MSR method is formulated as follows.

$$\min_{\mathbf{d},\mathbf{P}^t} f(\rho(\boldsymbol{\psi};\mathbf{d}))$$

$$s.t. \quad \mathbf{g}_{P_i^t} \cong \mathbf{g}_i(\rho(\boldsymbol{\psi};\mathbf{d}),\mathbf{x}(\mathbf{u}_i^t)) \geq 0, \quad i = 1, ..., n$$

$$P(E_{sys};\mathbf{P}^t) = \begin{cases} \int_{\mathbf{s}} \mathbf{c}^{\mathrm{T}}\mathbf{p}^t(\mathbf{s}) f_{\mathbf{S}}(\mathbf{s})d\mathbf{s} \leq P_{sys}^t & \text{dependent} \\ \mathbf{c}^{\mathrm{T}}\mathbf{p}^t \leq P_{sys}^t & \text{independent} \end{cases}$$

where $\mathbf{u}_i^t \cong \beta_i^t \cdot (\hat{\boldsymbol{\alpha}}_i^t)^{\mathrm{T}}$

$$\hat{\boldsymbol{\alpha}}_i^t \cong \left(-\frac{\nabla_{\mathbf{x}} g_i(\rho(\boldsymbol{\psi};\mathbf{d}),\mathbf{x}(\mathbf{u}))\mathbf{J}_{\mathbf{x},\mathbf{u}}}{\left\| \nabla_{\mathbf{x}} g_i(\rho(\boldsymbol{\psi};\mathbf{d}),\mathbf{x}(\mathbf{u}))\mathbf{J}_{\mathbf{x},\mathbf{u}} \right\|} \right)_{\mathbf{u}=\tilde{\mathbf{u}}_i} \quad (8)$$

When limit-states are statistically dependent, the system failure probability is defined as a function of design variables in $\mathbf{P}^t$ by constructing $\mathbf{p}(\mathbf{s})$ using $P_i(\mathbf{s})$ in (7) with β_i replaced by $\beta_i^t = -\Phi^{-1}(P_i^t)$. For a case with statistically independent limit-states, the probability vector $\mathbf{p}$ is constructed by use of $P_i^t = \Phi(-\beta_i^t)$. In (8), we denote the probability vectors by $\mathbf{p}^t$ and $\mathbf{p}^t(\mathbf{s})$ to indicate that the probability vectors are constructed by use of β_i^t instead of β_i. Inheriting the merits of the MSR method, the proposed SRBTO/MSR approach can evaluate the probability of a general system event efficiently and accurately with statistical dependence considered. This helps reduce the risk of having under- or over-conservative optimal designs caused by inaccurate system reliability calculations (Nguyen et al. 2010b).

The MSR method provides the parameter sensitivities of $P(E_{sys})$ with respect to design variables so as to facilitate the use of gradient-based optimization algorithms for SRBTO. From (5), the sensitivity of the system failure probability with respect to a parameter θ can be computed as follows.

$$\frac{\partial P(E_{sys})}{\partial \theta} = \begin{cases} \int_{\mathbf{s}} \mathbf{c}^{\mathrm{T}} \frac{\partial \mathbf{p}(\mathbf{s})}{\partial \theta} f_{\mathbf{S}}(\mathbf{s})d\mathbf{s} & \text{dependent} \\ \mathbf{c}^{\mathrm{T}} \frac{\partial \mathbf{p}}{\partial \theta} & \text{independent} \end{cases} \quad (9)$$

Song and Kang (2009) developed an efficient matrix procedure to construct $\partial \mathbf{p}/\partial \theta$ and $\partial \mathbf{p}(\mathbf{s})/\partial \theta$ from the parameter sensitivities of component probabilities $\partial P_i/\partial \theta$ and $\partial P_i(\mathbf{s})/\partial \theta$, respectively. For example, one can obtain component-level parameter sensitivities using the FORM (Bjerager and Krenk 1989).

Herein we derive the sensitivity of $P_i(\mathbf{s})$ with respect to the design variables in the proposed single-loop SRBTO,

P_i^t, $i = 1, \ldots, n$ so as to construct $\partial \mathbf{p}/\partial \theta$ and $\partial \mathbf{p}(\mathbf{s})/\partial \theta$ in (9) using the aforementioned matrix procedure in Song and Kang (2009). The sensitivity of $P_i(\mathbf{s})$ with respect to P_i^t is derived as

$$\frac{\partial P_i(\mathbf{s})}{\partial P_i^t} = \frac{\partial P_i(\mathbf{s})}{\partial \beta_i^t} \cdot \frac{\partial \beta_i^t}{\partial P_i^t} = -\frac{\partial P_i(\mathbf{s})}{\partial \beta_i^t} \cdot \frac{1}{\varphi(-\beta_i^t)} \quad (10)$$

in which $\varphi(\cdot)$ denotes the PDF of the standard normal distribution; and from (7), the sensitivity with respect to the target reliability index is derived as

$$\frac{\partial P_i(\mathbf{s})}{\partial \beta_i^t} = -\frac{1}{\sqrt{1 - \Sigma_{k=1}^m r_{ik}^2}} \varphi\left(\frac{-\beta_i^t - \Sigma_{k=1}^m(r_{ik}s_k)}{\sqrt{1 - \Sigma_{k=1}^m r_{ik}^2}} \right) \quad (11)$$

It is noted that the partial derivative of $P_i(\mathbf{s})$ with respect to $\mathbf{d}$ is zero (with P_i^t fixed). Therefore, for the constraint $P(E_{sys}) \leq P_{sys}^t$, it is not necessary to evaluate the sensitivity of $P(E_{sys})$ with respect to $\mathbf{d}$.

Next, the sensitivities of $g_{P_i^t} \cong g_i(\rho(\boldsymbol{\psi};\mathbf{d}),\mathbf{x}(\mathbf{u}_i^t))$ with respect to the design variables are derived as follows. First, the sensitivities with respect to design variables $\mathbf{d}$ are evaluated as

$$\frac{\partial g_i(\rho(\boldsymbol{\psi};\mathbf{d}),\mathbf{x}(\mathbf{u}_i^t))}{\partial \mathbf{d}} = \sum_{\rho} \frac{\partial g_i(\rho(\boldsymbol{\psi};\mathbf{d}),\mathbf{x}(\mathbf{u}_i^t))}{\partial \rho} \cdot \frac{\partial \rho(\boldsymbol{\psi};\mathbf{d})}{\partial \mathbf{d}} \quad (12)$$

where $\partial g_i(\rho,\mathbf{x})/\partial \rho$ is computed for the given limit-state definition, e.g. volume, compliance and displacement. For example, the adjoint method (Bendsøe and Sigmund 2003) may facilitate the sensitivity calculation; and $\partial \rho(\boldsymbol{\psi};\mathbf{d})/\partial \mathbf{d}$ is obtained from the given projection function (Nguyen et al. 2010a). The sensitivity of $g_{P_i^t}$ with respect to P_i^t is derived as

$$\frac{\partial g_{P_i^t}}{\partial P_i^t} = \left[\nabla_{\mathbf{u}} g_i(\rho(\boldsymbol{\psi};\mathbf{d}),\mathbf{x}(\mathbf{u})) \right]_{\mathbf{u}=\mathbf{u}_i^t} \frac{\partial \mathbf{u}_i^t}{\partial P_i^t}$$

$$\cong \left[\nabla_{\mathbf{x}} g_i(\rho(\boldsymbol{\psi};\mathbf{d}),\mathbf{x}(\mathbf{u})) \cdot \mathbf{J}_{\mathbf{x},\mathbf{u}} \right]_{\mathbf{u}=\mathbf{u}_i^t} \frac{\partial \beta_i^t}{\partial P_i^t}(\hat{\boldsymbol{\alpha}}_i^t)^{\mathrm{T}}$$

$$= -\frac{1}{\varphi(-\beta_i^t)} \left[\nabla_{\mathbf{x}} g_i(\rho(\boldsymbol{\psi};\mathbf{d}),\mathbf{x}(\mathbf{u})) \cdot \mathbf{J}_{\mathbf{x},\mathbf{u}} \right]_{\mathbf{u}=\mathbf{u}_i^t} (\hat{\boldsymbol{\alpha}}_i^t)^{\mathrm{T}} \quad (13)$$

Note that this partial derivative is approximate because $\hat{\boldsymbol{\alpha}}_i^t$ is assumed to be insensitive to the changes in P_i^t during the design iterations.

3 Improving accuracy of component and system reliability-based topology optimization

This section introduces new single-loop approaches to improve the accuracy of reliability calculations in component and system RBTO problems with highly nonlinear limit-state functions.

3.1 Accuracy in FORM-based reliability-based design and topology optimization

As shown in (2), (4) and (8), the system reliability analysis during an SRBTO employs the results from the component reliability analyses on the given limit-states. Therefore, the accuracy of SRBTOs in satisfying the probabilistic constraint on the system event, i.e. $P(E_{sys}) \leq P_{sys}^t$, depends on that of the component reliability analyses. The inaccuracy of the FORM-based reliability-based design and topology optimization has been reported in the literature (Mogami et al. 2006; Royset et al. 2006; McDonald and Mahadevan 2008; Rahman and Wei 2008; Silva et al. 2010; Lee et al. 2010). Some studies have been conducted to improve the accuracy. For example, Royset et al. (2006) employed the first-order approximation for failure probability and then used higher-order reliability approximations or Monte Carlo simulations to adjust parameters to improve the accuracy of system reliability-based design optimization. Lee et al. (2010) proposed to use the MPP-based dimension reduction method (Xu and Rahman 2005) in the SRBDO framework.

Most of the single-loop SRBDO and SRBTO approaches (Liang et al. 2007; McDonald and Mahadevan 2008; Nguyen et al. 2010b; Silva et al. 2010) also employ the FORM for component probability analyses, which potentially results in unconservative or non-optimal solutions when the limit-state functions are highly nonlinear. For example, if a limit-state function is defined in term of the compliance under uncertain loads, the function is a quadratic function of the random variables representing the uncertainty in the loads. Therefore, the linear approximation by FORM may cause significant errors in component reliability analyses, and thus also in system reliability calculations. As an effort to apply the single-loop approach to a wide range of topology optimization problems, we propose a method to enhance the accuracy of the failure probabilities calculated during the single-loop component and system RBTO.

3.2 Single-loop component reliability design and topology optimization with improved accuracy

First, let us consider the single-loop CRBTO approach in (3). At each step of the design iterations, the approximate location for the performance function value $\mathbf{u}_i^t$ is obtained by scaling the negative normalized gradient vector $\hat{\boldsymbol{\alpha}}_i^t$ evaluated at the point obtained from the KKT condition, $\mathbf{u} = \tilde{\mathbf{u}}_i$ by the target reliability index β_i^t, i.e. $\mathbf{u}_i^t \cong \beta_i^t \cdot (\hat{\boldsymbol{\alpha}}_i^t)^{\mathrm{T}}$. The validity of this approximate location for the performance function value $\mathbf{u}_i^t$ is checked at the final step of the design iterations. We modify this procedure to improve the accuracy of the single-loop approach. Instead of finding the approximate location for the performance function value on the surface of the sphere with the fixed radius β_i^t, the radius is updated at each step of the design iterations by the ratio of β_i^t to the reliability index improved based on the curvatures at the approximate location for the performance function value $\mathbf{u}_i^t$ of the previous step. The formulation of the proposed scheme is as follows.

$$\min_{\mathbf{d}} f(\rho(\boldsymbol{\psi}; \mathbf{d}))$$

$$s.t. \quad \mathrm{g}_{P_i^t} \cong \mathrm{g}_i(\rho(\boldsymbol{\psi}; \mathbf{d}), \mathbf{x}(\mathbf{u}_i^t)) \geq 0, \quad i = 1, ..., n$$

at the k-th step: $\mathbf{u}_i^t \cong \beta_i^{t(k)} \cdot (\hat{\boldsymbol{\alpha}}_i^t)^{\mathrm{T}}$

$$\beta_i^{t(k)} = \begin{cases} \beta_i^t & k = 1 \\ \dfrac{\beta_i^t}{\beta_i^{t(k-1)(SORM)}} \times \beta_i^{t(k-1)} & \text{otherwise} \end{cases}$$

$$\hat{\boldsymbol{\alpha}}_i^t \cong \left(-\frac{\nabla_{\mathbf{x}} g_i(\rho(\boldsymbol{\psi}; \mathbf{d}), \mathbf{x}(\mathbf{u})) \mathbf{J}_{\mathbf{x}, \mathbf{u}}}{\left\| \nabla_{\mathbf{x}} g_i(\rho(\boldsymbol{\psi}; \mathbf{d}), \mathbf{x}(\mathbf{u})) \mathbf{J}_{\mathbf{x}, \mathbf{u}} \right\|} \right)_{\mathbf{u} = \tilde{\mathbf{u}}_i}$$

(14)

where $\beta_i^{t(k)}$ is the target reliability index used to find the approximate location for the performance function value at the k-th step of the iterations; and $\beta_i^{t(k-1)(SORM)}$ is the reliability index of the $(k-1)$-th step which was improved based on the curvatures of the limit-state function at the approximate location for the performance function value as follows

$$\beta_i^{t(k-1)(SORM)} = -\Phi^{-1}\left(P_i^{t(k-1)(SORM)}\right)$$

$$P_i^{t(k-1)(SORM)} = \Phi\left(-\beta_i^{t(k-1)}\right) \prod_{j=1}^{m-1} \frac{1}{\sqrt{1 + \kappa_j \beta_i^{t(k-1)}}} \quad (15)$$

in which $P_i^{t(k-1)(SORM)}$ denotes the failure probability estimated by use of the approximate location for the performance function value $\mathbf{u} = \mathbf{u}_i^t$ at the $(k-1)$-th step by the concept of the second-order reliability method (SORM; Breitung 1984; Der Kiureghian 2005); and κ_j ($j = 1, \ldots, m-1$) denote the principal curvatures around the approximate location for the performance function value at the $(k-1)$-th step, $\mathbf{u} = \mathbf{u}_i^t$. Figure 1 shows the actual MPP $\mathbf{u}^*$ of the given design and the approximate location for the performance function value $\mathbf{u}^t$ where the improved reliability index $\beta_i^{t(k-1)(SORM)}$ is computed using Breitung's
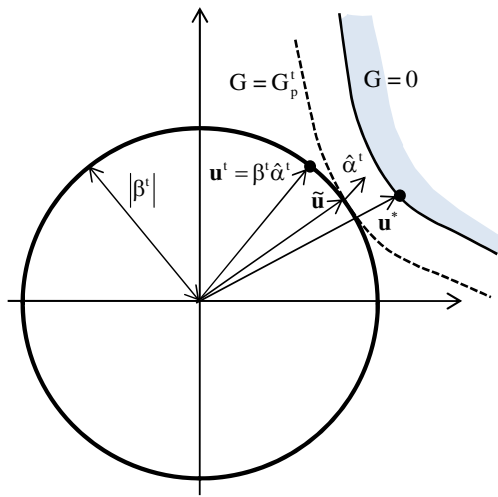
Fig. 1 Actual MPP ($\mathbf{u}^*$) and approximate location for the performance function value ($\mathbf{u}^t$)

formula in (15). The convergence of the radius $\beta_i^{t(k)}$ indicates that the SORM-based reliability index approaches the target reliability index β_i^t. Compared to similar techniques in the literature (Royset et al. 2006; Rahman and Wei 2008; Lee et al. 2010), our study focuses on implementation of SORM into the *single-loop* RBTO. In this study, the improved CRBTO by SORM in (14) is termed as "SORM-based CRBTO." It should be noted that other reliability analysis methods than SORM, such as importance sampling method or dimension reduction method can be used for the updating rule in the proposed approach if necessary.

3.3 Single-loop system reliability-based design and topology optimization with improved accuracy

The single-loop SRBTO/MSR in (8) is also improved by enhancing the accuracy of component reliability analysis results that are used for system reliability analyses. The formulation of the SORM-based SRBTO/MSR is as follows

$$\min_{\mathbf{d}, \mathbf{P}^t} f(\rho(\boldsymbol{\psi}; \mathbf{d}))$$

$$s.t. \quad g_{P_i^t} \cong g_i(\rho(\boldsymbol{\psi}; \mathbf{d}), \mathbf{x}(\mathbf{u}_i^t)) \geq 0 \quad i = 1, ..., n$$

$$P\left(E_{sys}; \mathbf{P}^{t(SORM)}\right)$$

$$= \begin{cases} \int_{\mathbf{s}} \mathbf{c}^{\mathrm{T}} \mathbf{p}^{t(SORM)}(\mathbf{s}) f_{\mathbf{S}}(\mathbf{s}) d\mathbf{s} \leq P_{sys}^t & \text{dependent} \\ \mathbf{c}^{\mathrm{T}} \mathbf{p}^{t(SORM)} \leq P_{sys}^t & \text{independent} \end{cases}$$

where $\mathbf{u}_i^t \cong \beta_i^t \cdot (\hat{\boldsymbol{\alpha}}_i^t)^{\mathrm{T}}$

$$\hat{\boldsymbol{\alpha}}_i^t \cong \left(-\frac{\nabla_{\mathbf{x}} g_i(\rho(\boldsymbol{\psi}; \mathbf{d}), \mathbf{x}(\mathbf{u})) \mathbf{J}_{\mathbf{x}, \mathbf{u}}}{\|\nabla_{\mathbf{x}} g_i(\rho(\boldsymbol{\psi}; \mathbf{d}), \mathbf{x}(\mathbf{u})) \mathbf{J}_{\mathbf{x}, \mathbf{u}}\|} \right)_{\mathbf{u} = \tilde{\mathbf{u}}_i}$$

$$(16)$$

where $\mathbf{P}^{t(SORM)}$ is the vector of the component failure probabilities by Breitung's formula (15) at the approximate location for the performance function values, $\mathbf{u}_i^t$, $i = 1, ..., n$; $\mathbf{p}^{t(SORM)}(\mathbf{s})$ and $\mathbf{p}^{t(SORM)}$ denote the probability vector constructed by use of the Breitung's formula reliability indexes $\beta_i^{t(SORM)}$ instead of β_i^t; and $\tilde{\mathbf{u}}_i$ is obtained by use of the KKT condition using β_i^t. The only change from (8) is that the probability vector is constructed by use of the SORM-based reliability indexes instead of the FORM reliability indexes at the approximate location for the performance function values.

4 Multiresolution Topology Optimization (MTOP)

A main challenge in performing RBTOs for realistic problems is the high computational cost which is inherited from deterministic topology optimization. The material distribution method (Bendsøe 1989) is often used in topology optimization. This method rasterizes the domain via the density of pixels/voxels, and thus often requires a large number of design variables, especially in three-dimensional applications. Most of the research efforts to overcome this challenge focused on finite element analysis that constitutes the dominant computational cost in topology optimization. For example, researchers make use of powerful computing resources such as parallel computing (Borrvall and Petersson 2001; Evgrafov et al. 2008), approximation procedure (Amir et al. 2009), or fast iterative solvers (Wang et al. 2007; Amir et al. 2010). These studies employ the same level of resolutions for finite element mesh and the design mesh during optimization process. In order to obtain high resolution topology designs with a relatively low computational cost, we hereby propose to employ a recently developed multiresolution topology optimization approach (Nguyen et al. 2010a) for SRBTO problems. In this section, the MTOP approach is introduced and further developed to include pattern symmetry and pattern repetition constraints.

4.1 MTOP formulation

To illustrate the MTOP approach, let us consider a "minimum compliance" topology optimization problem:

$$\min_{\mathbf{d}} f(\rho(\boldsymbol{\psi}; \mathbf{d})) = C(\rho(\boldsymbol{\psi}; \mathbf{d}), \mathbf{u}_d) = \mathbf{f}^{\mathrm{T}} \mathbf{u}_d$$

$$s.t. \quad V(\rho(\boldsymbol{\psi}; \mathbf{d})) = \int_{\Omega} \rho(\boldsymbol{\psi}; \mathbf{d}) dV \leq V_s \qquad (17)$$

where $C(\rho, \mathbf{u}) = \mathbf{f}^{\mathrm{T}} \mathbf{u}_d$ is the compliance of the continuum; $V(\rho)$ is the total volume; and V_s is the prescribed volume constraint. A desirable solution of topology optimization

specifies the density at every point in the domain as either 0 (void) or 1 (solid). However, since it is impractical to perform such an integer optimization, the problem is relaxed such that the density can have any value between 0 and 1. For example, in the Solid Isotropic Material with Penalization (SIMP) approach (Bendsøe 1989; Rozvany et al. 1992), the constitutive matrix is parameterized using solid material density as follows

$$\mathbf{D}(\boldsymbol{\psi}) = \rho(\boldsymbol{\psi}; \mathbf{d})^p \mathbf{D}^0 \tag{18}$$

where $\mathbf{D}^0$ is the constitutive matrix of the material in the solid phase, corresponding to the density $\rho(\boldsymbol{\psi}; \mathbf{d}) = 1$; and p is the penalization parameter. To prevent singularity of the stiffness matrix, a small positive lower bound, e.g. $\rho_{min} = 10^{-3}$, is placed on the density. Using the penalization parameter $p > 1$, the intermediate density approaches either 0 (void) or 1 (solid). In the conventional element-based approach, the density of each element is represented by one value ρ_e. In this case, the global stiffness matrix $\mathbf{K}$ in (1) is expressed as

$$\mathbf{K} = \sum_{e=1}^{N_{el}} \mathbf{K}_e(\rho_e) = \sum_{e=1}^{N_{el}} \int_{\Omega_e} \mathbf{B}^T \mathbf{D}(\rho_e) \mathbf{B} \, d\Omega \tag{19}$$

where $\mathbf{K}_e(\rho_e)$ is the stiffness matrix of the element e; $\mathbf{B}$ is the strain-displacement matrix of shape function derivatives; Ω_e denotes the domain of the element e; and $\mathbf{D}(\rho_e)$ is the constitutive matrix in the element determined by the density ρ_e.

Different from the conventional approaches that use the same mesh for finite element analysis and design (Fig. 2a), the MTOP approach utilizes three different meshes: a *relatively coarse finite element (FE) mesh* to perform the analysis, a *fine design variable mesh* to perform the opti-

mization, and a *fine density mesh* to represent material distribution and compute the stiffness matrices. The density mesh is finer than the finite element mesh so that each finite element consists of a number of density elements (sub-elements). Within each density element, the material density is assumed to be uniform. For example, Fig. 2a shows a conventional element-based approach Q4/U element while Fig. 2b shows an MTOP Q4/n25/d25 element where "n25" and "d25" respectively indicate that the number of density elements and design variable per a Q4 element is 25.

The MTOP approach needs a scheme to obtain the element stiffness matrix from corresponding density elements and design variables. The stiffness matrix is computed as the summation of the integration of the stiffness integrand over each density element, which has uniform density. As a result, the formulation for the stiffness matrix integration is expressed as follows.

$$\mathbf{K}_e = \int_{\Omega_e} \mathbf{B}^T \mathbf{D} \mathbf{B} \, d\Omega = \int_{-1}^{1} \int_{-1}^{1} \mathbf{B}^T \mathbf{D} \mathbf{B} J \, d\xi d\eta$$

$$= \sum_{i=1}^{n} \left((\rho_i)^p \int_{\Omega_i^0} \mathbf{B}^T \mathbf{D}^0 \mathbf{B} J \, dA_i^0 \right) = \sum_{i=1}^{n} (\rho_i)^p \mathbf{I}_i$$

$$\mathbf{I}_i = \int_{\Omega_i^0} \mathbf{B}^T \mathbf{D}^0 \mathbf{B} J \, dA_i^0 \tag{20}$$

where ξ, and η denote the intrinsic coordinates in the interval $[-1,1]$; J is the Jacobian; A_i^0 is the area/volume of each density element i in the reference domain Ω_i^0; and ρ_i is the density in the i-th density element. The solution of the optimization problem in (17) by a gradient-based optimizer would require the computation of sensitivities of objective function and constraint. The sensitivities of the compliance and the volume with respect to design variables are derived as follows.

$$\frac{\partial C}{\partial d_n} = \sum_{\rho_i} \frac{\partial C}{\partial \rho_i} \frac{\partial \rho_i}{\partial d_n} = \sum_{\rho_i} -\mathbf{u}^T \frac{\partial \mathbf{K}}{\partial \rho_i} \mathbf{u} \frac{\partial \rho_i}{\partial d_n}$$

$$\frac{\partial V}{\partial d_n} = \sum_{\rho_i} \frac{\partial V}{\partial \rho_i} \frac{\partial \rho_i}{\partial d_n} \tag{21}$$

where the sensitivity $\partial \mathbf{K}/\partial \rho_i$ can be derived from (20) and (21) (Bendsøe and Sigmund 2003; Nguyen et al. 2010a). The sensitivities of the density with respect to design variables depend on the definition of the material density function. The MTOP approach utilizes a projection method (Guest et al. 2004) to compute the density of each density element from the design variables via a projection function $f_p(.)$. The projection method also provides the mesh independence and minimum length scale for the topology design (Nguyen et al. 2010a). For example, if a linear projection method is employed, the uniform density of a density
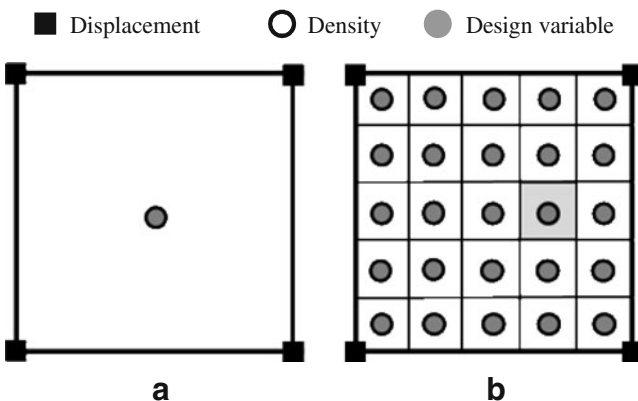

Displacement   ○ **Density**   ● **Design variable**

Fig. 2 Element-based and MTOP elements: **a** Q4/U; and **b** MTOP Q4/n25/d25

element, ρ_i is computed as the weighted average of the design variables in the neighborhood, i.e.

$$\rho_i = \frac{\sum_{n \in S_i} d_n \cdot w(r_{ni})}{\sum_{n \in S_i} w(r_{ni})},$$

where $w(r_{ni}) = \begin{cases} \dfrac{r_{\min} - r_{ni}}{r_{\min}} & \text{if } r_{ni} \leq r_{\min} \\ 0 & \text{otherwise} \end{cases}$ (22)

where d_n denotes the n-th design variable; S_i is the subdomain corresponding to the i-th density element; and r_{ni} is the distance from the point associated with design variable d_n to the centroid of the i-th density element, i.e. $r_{ni} = \|\boldsymbol{\psi}_n - \boldsymbol{\psi}_{ni}\|$ in which $\boldsymbol{\psi}_n$ and $\boldsymbol{\psi}_{ni}$ are the coordinates of the point associated with design variable d_n and S_i, respectively. Here it is assumed that the change of material density occurs over the physical radius $r_{\min}$, which is independent of mesh. Using the projection function with a minimum length scale, the mesh independent solution is obtained. In this study, the method of moving asymptotes (MMA; Svanberg 1987) is used as the gradient-based optimizer. The MTOP approach is used in all numerical examples of the reliability-based topology optimization in this paper. Various two- and three-dimensional problems demonstrated that the MTOP approach can achieve high resolution optimal topologies with relatively low computational cost in comparison to the conventional element-based approach (Nguyen 2010, Nguyen et al. 2010a). The approach can promote high-resolution topology optimization in various problems including biomedical problems, e.g. optimal design of craniofacial segmental bone replacements (Sutradhar et al. 2010).

4.2 Pattern symmetry and pattern repetition in MTOP

The topology optimization approach is usually applied to concept design of structures. Due to some practical design constraints or demands, these structures may require pattern symmetry and/or pattern repetition in the design. For example, pattern symmetry and repetition have been successfully incorporated into the topology optimization of functionally graded material in two-dimensional structures (Almeida et al. 2010). In this study, we implement pattern symmetry and repetition conditions into the framework of the multiresolution topology optimization. Because the design variables are separated from the analysis model in the MTOP framework, we can choose a basic set of design variables and map to the whole domain to satisfy the pattern symmetry and/or pattern repetition condition. Figure 3 illustrates the mapping schemes to gain pattern symmetry and repetition in the optimal design.
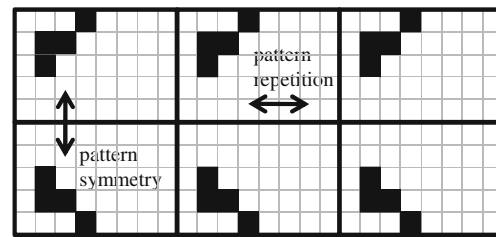

Fig. 3 Design variables mapping for pattern symmetry and pattern repetition

5 Numerical examples

In this section, the proposed SRBTO/MSR procedure and the SORM-based improvement on CRBTO and SRBTO/MSR are demonstrated by numerical examples. In all numerical examples, MTOP is used for computational efficiency. First, a two-dimensional bridge example demonstrates the impact of statistical dependence between the limit-states in SRBTO, which can be taken into account by the SRBTO/MSR approach. Second, a three-dimensional cube example shows the improvement in the accuracy of the SORM-based RBTOs over the traditional FORM-based RBTOs. Third, a three-dimensional building example demonstrates that the SORM-based SRBTO approach can be applied to computationally demanding topology optimization problems with pattern repetition scheme by use of the MTOP approach. For simplicity, all the quantities are given dimensionless.

5.1 Two-dimensional bridge

Consider a two-dimensional bridge design in a domain of 250×50 and thickness of 0.05 as shown in Fig. 4. The objective of the optimal design is to minimize the volume of the structure under constraints on the displacements at selected locations. The isotropic material is assumed to have Young's modulus E^0 of 2×10^8 and Poisson's ratio ν of 0.3. The minimum length scale $r_{\min} = 1.25$, and penalization parameter $p = 3$ are employed. These material properties are hereby assumed to be deterministic since the uncertainties in material properties usually have minimal impacts on reliability-based optimal topologies for a structure under linear elastic behavior. Stochastic loads are applied at nine locations on a non-designable layer (with thickness of two)
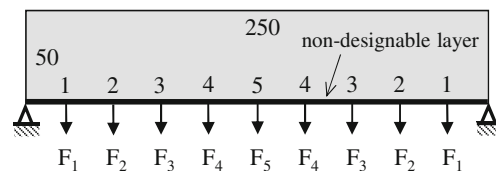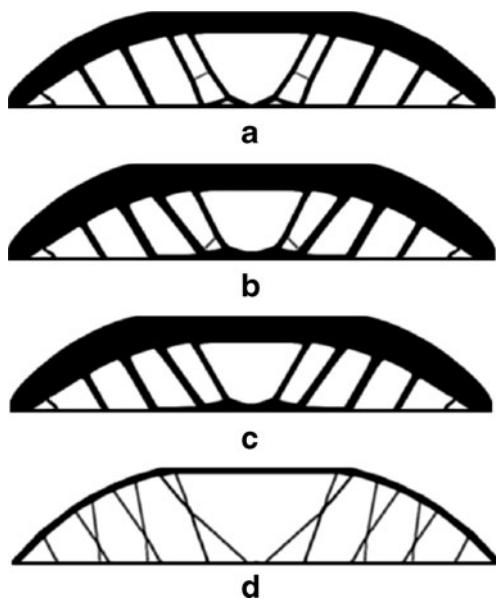

Fig. 4 Configuration of two-dimensional bridge example

Fig. 5 The results of two-dimensional bridge example: **a** DTO ($\mu_F = 10^5$, *volfrac* = 39.07%); **b** FORM-based CRBTO ($\mu_F = 10^5$, *volfrac* = 48.64%); **c** FORM-based SRBTO/MSR ($\mu_F = 10^5$, *volfrac* = 47.70%); and **d** FORM-based SRBTO/MSR ($\mu_F = 2.5 \times 10^4$, *volfrac* = 16.66%)

at the bottom of the bridge as shown in Fig. 4. A symmetric loading condition is assumed, so the nine loads are modeled by use of five random variables. Each of the five random variables is assumed to follow a Gaussian distribution with the mean (μ_F) of 100,000 and coefficient of variation (ratio of the standard deviations to the means) of 1/6. All the five random variables are assumed to be uncorrelated. The constraints on the displacements at the locations of the applied forces are described by the limit-state functions

$$g_i\left(\boldsymbol{\rho}, \mathbf{F}\right) = d_i^0 - d_i\left(\boldsymbol{\rho}, \mathbf{F}\right), \ i = 1, .., 5 \tag{23}$$

where $\boldsymbol{\rho}$ denotes the vector of the element densities; $\mathbf{F}$ is the vector of the five random variables representing applied forces; $d_i(\boldsymbol{\rho}, \mathbf{F})$ is the vertical displacement at the i-th location predicted by a finite element analysis; and d_i^0 is the limit on the displacement. In this example, the displacement limits are given as $\{d_i^0\}_{i=1,..,5} = \{1.25, 1.50, 1.75, 2.00, 2.25\}$. Because of the symmetry

conditions, only a half of the domain is taken into the analysis model with 125×50 MTOP elements (Q4/n9/d9).

First, a deterministic topology optimization (DTO) is performed with the loads equal to the given mean values. This is performed by (1) except that the probabilistic constraints are replaced by deterministic ones, i.e. $g_i(\boldsymbol{\rho}, \mathbf{F}) \geq 0$. The corresponding optimal design is shown in Fig. 5a. The volume fraction (*volfrac*) of the optimal design, i.e. the ratio of the optimal volume to that of the original domain is 39.07%. Next, a FORM-based CRBTO is conducted as in (3) with all the reliability index targets $\beta_i^t = 2$ (or $P_i^t = 0.02275$). The optimal topology shown in Fig. 5b has the volume fraction of 48.64%. This optimal volume is higher than that by the DTO since the topology that avoids the failure under the mean loads is expected to have significantly higher probability to violate the constraints than the given target failure probability. After the CRBTO optimization is completed, the probability that at least one of the constraints is violated (i.e. series system) is estimated by the MSR method as $P_{sys} = 0.066517$. Next, a FORM-based SRBTO/MSR is performed for the series system event with the target system failure probability $P_{sys} = 0.066517$, which was chosen to be the same as the system failure probability of the optimal topology by the CRBTO in order to compare the optimal topologies by CRBTO and SRBTO that have the same system failure probability. The SRBTO optimal topology, which is different from those by DTO and CRBTO, is shown in Fig. 5c (volume fraction of 47.70%). Another SRBTO is performed with the mean values of the random loads reduced to 25% (Fig. 5d) to investigate the impacts of the load intensity on the optimal topology.

Table 1 shows the component and system failure probabilities by Monte Carlo simulations (MCS) for the optimal designs by the CRBTO and SRBTO in order to verify the accuracy of the FORM-based RBTO procedures in this example. The results confirm that the FORM-based RBTO designs provide failure probabilities that are compatible with the target probabilities on component events (CRBTO) and system event (SRBTO). This is because the limit-state functions in this example are linear function of the uncertain loads and the random variables are assumed to follow Gaussian distributions. Thus, the improvement schemes proposed in Section 3 is not needed.

Table 1 Two-dimensional bridge example: verification of failure probabilities of CRBTO and SRBTO designs by MCS (10^6 times, c.o.v = 0.005)

	CRBTO	MCS on CRBTO design	SRBTO/MSR	MCS on SRBTO design
P_1	0.002275	0.002266	0.001214	0.001281
P_2	0.002275	0.022798	0.016284	0.016331
P_3	0.002275	0.023119	0.039239	0.039377
P_4	0.002275	0.023019	0.042740	0.042662
P_5	0.002275	0.023132	0.023450	0.023239
P_{sys}	0.066517	0.066990	0.066517	0.066719

The efficiency of MTOP over the conventional element-based approach is investigated by using the SRBTO problem above. To obtain a similar level of resolution using the element-based approach, it is necessary to use 375×150 Q4/U elements. After 50 iterations, the computer run time of the element-based approach is about two times more than the MTOP Q4/n9/d9 approach. The relative efficiency is further increased as we aim at a higher level of resolution. More details on comparison of computational costs are found in (Nguyen 2010; Nguyen et al. 2010a).

In this example, the volume fraction from SRBTO (47.70%) is fairly close to that of the CRBTO (48.64%) that gives the same system failure probability. This might give an impression that it is not necessary to perform SRBTO considering the additional computations for the system failure probability. However, SRBTO is still preferred for RBTO problems when probabilistic constraint is given on the system failure event for the following reasons. First of all, the probabilistic constraints on individual limit-states that would satisfy the given constraint on the system failure probability are not known a priori. In this numerical example, we chose the constraint on the system failure probability in SRBTO as the system failure probability of the result of the CRBTO just for comparison purpose. Second, in using CRBTO formulation for solving SRBTO problems, all the component target failure probabilities are often given equal mainly because the actual component failure probabilities of an optimal design that would satisfy the system constraint are not known. Introducing such uniform target component failure probabilities often makes the SRBTO problems more constrained than necessary, which may lead to non-optimal solutions (Nguyen et al. 2010b). Finally, in SRBTO, one can identify the relative contribution of each limit-state to the system probability based on components probabilities of the optimal design or by use of the component importance measures by the MSR method (Song and Kang 2009; Nguyen et al. 2010b). According to the component failure probabilities of the optimal designs, the importance ranking of the limit-states is as follows: 4 (most important) $\rightarrow 3 \rightarrow 5 \rightarrow 2 \rightarrow 1$ (least important).

The effects of the mean values, coefficient of variations, and the correlations between random variables $F_i's$ on the optimal topologies are also investigated. For simplicity, all the loads are assumed to have the same mean values (μ_F), coefficients of variation (c.o.v), and correlation coefficients (ρ_{ij}). The SRBTO problem is solved again with the same target system probability of 0.066517 while the mean values, coefficients of variation and correlation coefficients are varied. First, Fig. 6a and b show that the increase in mean values (from 0.25×10^5 to 1.25×10^5) and coefficients of variation (from 0.01 to 0.50) results in the increase in volume fractions of the optimal topologies. Next, the impacts of changes in the correlation coefficients (from 0.00 to
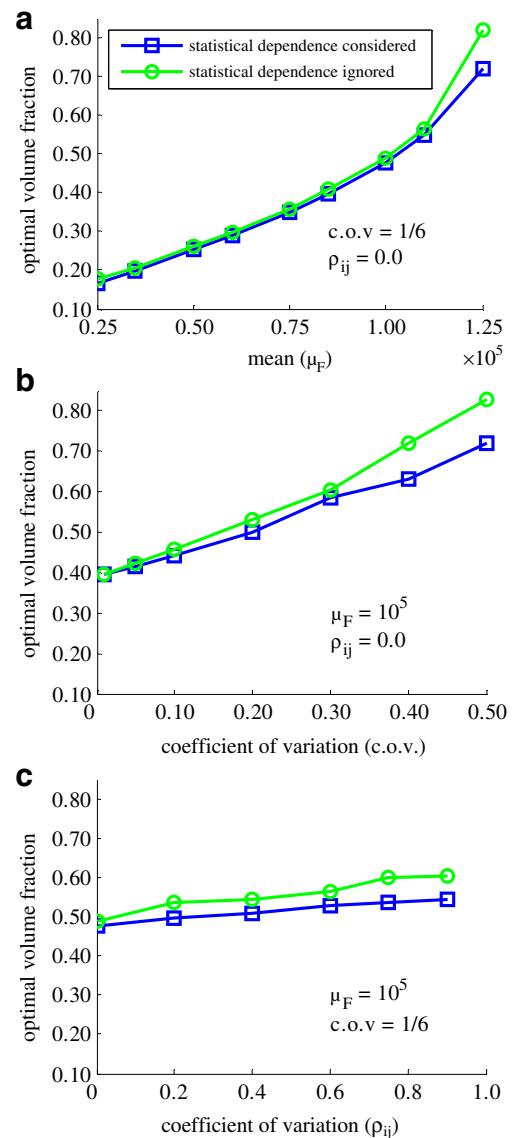

Fig. 6 Impact on FORM-based SRBTO results (volume fraction) by changes in **a** mean values (c.o.v = 1/6, $\rho_{ij} = 0.0$); **b** coefficients of variation ($\mu_F = 100,000$, $\rho_{ij} = 0.0$); and **c** correlation coefficients ($\mu_F = 100,000$, c.o.v = 1/6) of the load random variables

0.90) of the load random variables are shown in Fig. 6c. It is seen that positive correlation among the random loads results in higher volume fractions, i.e. more conservative design. This is because positively correlated loads increase the displacements, and thus the failure probabilities. Therefore, in this problem, if the positive correlation is ignored, the RBTO may lead to an unsafe design. Also presented in each plot are the results with the statistical dependence between limit-states ignored, i.e. each joint probability can be computed by the product of the component probabilities (Nguyen 2010; Silva et al. 2010). As shown in Fig. 6, designs become more conservative than necessary when statistical dependence is ignored. This is because the failure

probability of a series system is overestimated when statistical dependence is ignored. Figure 6b and c show that the effect of statistical dependence on the optimal designs increases as the coefficients of variation or the correlation coefficients of the random loads increase.

5.2 Three-dimensional cube

This numerical example is to demonstrate the improved accuracy of the proposed SORM-based RBTO methods. The objective of optimization is to minimize the volume in a cube domain shown in Fig. 7 while satisfying deterministic or probabilistic constraints on the compliances for multiple load cases. One corner is fixed in all three directions while the other corners are restricted in the vertical direction only. The isotropic material is assumed to have Young's modulus of $E^0 = 1{,}000$ and Poisson's ratio of $\nu = 0.3$. A cube with edge length $L = 24$ is divided into $12 \times 12 \times 12$ B8/n125/d125 MTOP elements with a total of 216,000 density elements. The minimum length scale $r_{min} = L/10$, and penalization parameter $p = 3$ are employed. The structure is subjected to three random loads applied at five locations as shown in Fig. 7. F_1 denotes the magnitude of the force at the center while F_2 and F_3 represent the loads at the midpoints between the center and the four corner points of the top face. F_1, F_2 and F_3 are assumed to be normal random variables with the mean values 100, 0 and 0, and with the standard deviations 10, 30 and 40, respectively.

Limit-states are defined on the compliances caused by two load combinations $\overline{\mathbf{F}}_1 = (F_1, F_2)$ and $\overline{\mathbf{F}}_2 = (F_1, F_3)$ as follows.

$$g_i\left(\boldsymbol{\rho}, \overline{\mathbf{F}}_i\right) = C_i^t - C_i\left(\boldsymbol{\rho}, \overline{\mathbf{F}}_i\right) = C_i^t - \mathbf{u}^{\mathrm{T}}\mathbf{F}_i, \ i = 1, 2 \quad (24)$$

where $C_i^t(= 120)$ is the threshold value on the compliance; $C_i(\boldsymbol{\rho}, \overline{\mathbf{F}}_i)$ is the compliance corresponding to the load case
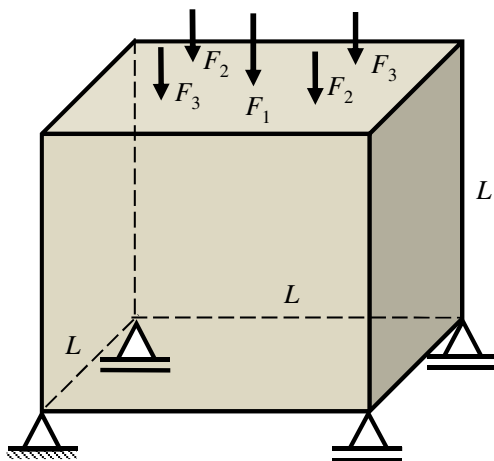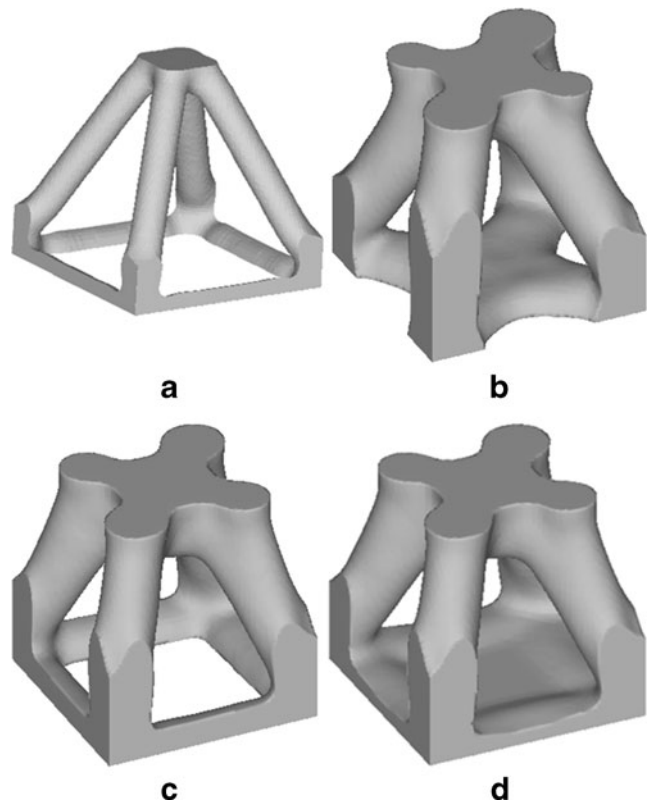

Fig. 8 Optimal topologies by **a** DTO (*volfrac* = 6.3%); **b** SORM-based CRBTO ($\sigma(F_1) = 10$, *volfrac* = 24.4%); **c** SORM-based SRBTO ($\sigma(F_1) = 10$, *volfrac* = 22.3%); and **d** SORM-based SRBTO ($\sigma(F_1) = 20$, *volfrac* = 23.9%)

$\overline{\mathbf{F}}_i$; and $\mathbf{F}_i$ is the global force vector assembled based on the load case $\overline{\mathbf{F}}_i$. The following three topology optimization problems are investigated: (1) Deterministic Topology Optimization (DTO) using the mean values of the loads with deterministic constraints $g_i(\boldsymbol{\rho}, \overline{\mathbf{F}}_i) \geq 0$; (2) CRBTO with probability constraints $P_1^t = P_2^t = 0.02275$, i.e. reliability indexes $\beta_1^t = \beta_2^t = 2.0$; and (3) SRBTO with the system limit-state $E_{sys} = \{(g_1(\boldsymbol{\rho}, \overline{\mathbf{F}}_1) \leq 0) \cup (g_2(\boldsymbol{\rho}, \overline{\mathbf{F}}_2) \leq 0)\}$ with

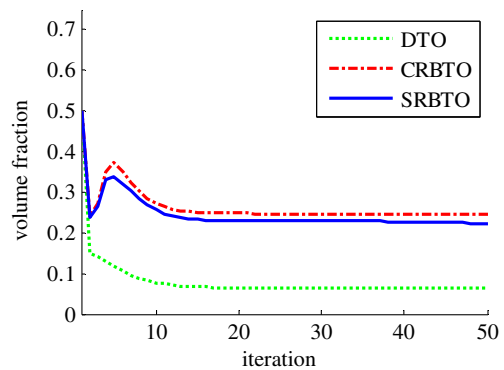**Fig. 7** Three-dimensional topology optimization of a cube

Fig. 9 Convergence histories of topology optimizations of a three-dimensional cube

$P_{sys}^t = 0.04493$, which is given so as to match the system failure probability of the optimal topology of the CRBTO.

Figure 8 shows the optimal topologies by DTO (Fig. 8a), SORM-based CRBTO (Fig. 8b), and SORM-based SRBTO (Fig. 8c). The volume fraction of DTO is lower than CRBTO and SRBTO because the risk of high compliance caused by the load uncertainties is ignored. It is noteworthy that, with the same system failure probabilities, the volume fraction of CRBTO is 10% higher than SRBTO. This is because CRBTO approach (assigning fixed constraints on individual components) is generally more constrained

than SRBTOs (assigning a constraint on system event, not on the individual components) at the same level of system failure probability (Nguyen et al. 2010b). Figure 8d shows the result of the SRBTO with the standard deviation of F_1 increased to 20 in order to see the impact of the load variability on the optimal topology. In summary, it is seen from Fig. 8 that the optimal topology is affected significantly by the load variability and the failure event definitions on the optimal topology of a structure.

The convergence histories of the optimizations are shown in Fig. 9. The proposed single-loop SORM-based CRBTO
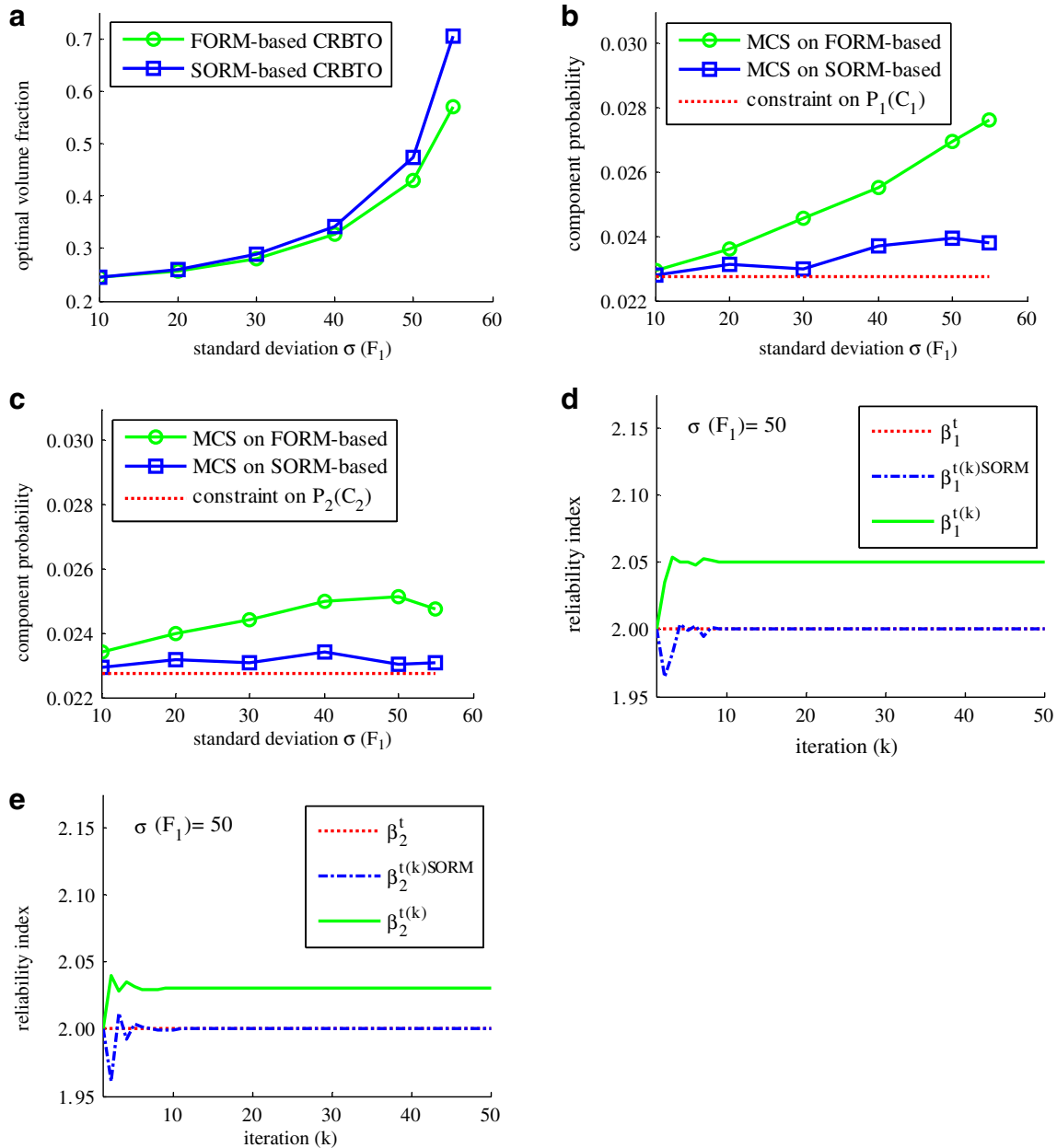

Fig. 10 CRBTOs with standard deviation of load F_1: **a** volume fraction of optimal designs; **b** failure probabilities of the first limit-state; **c** failure probabilities of the second limit-state; **d** reliability index con-vergence for the first limit-state with standard deviation $\sigma(F_1) = 50$; and **e** reliability index convergence for the second limit-state with standard deviation $\sigma(F_1) = 50$

and SRBTO show similar rates of convergence, which are also comparable to that of DTO. The system failure probability of the optimal topology found by SORM-based SRBTO/MSR, $P_{sys} = 0.04493$ is verified by a fairly close estimate by MCS, $P_{sys} = 0.04515$ (10^6 times, c.o.v = 0.005).

In order to demonstrate the improved accuracy of the SORM-based single-loop CRBTO method, the results are compared with those by the FORM-based CRBTO with the component probability targets $P_1^t = P_2^t = 0.02275$. Figure 10a shows the difference in the volume fractions of the optimal designs. Monte Carlo simulations (MCS: 10^6 times, c.o.v = 0.005) are performed to find the component failure probabilities of the optimal topologies by the FORM-based and SORM-based CRBTOs. The results in Fig. 10b and c show that the component probabilities of SORM-based CRBTOs are fairly close to the target probabilities while the FORM-based CRBTOs show significant errors especially when the random loads have large variability. In addition, Fig. 9d and e show the convergence histories of the reliability indexes of the first and second limit states, respectively, for the standard deviation load F_1, $\sigma(F_1) = 50$. It is observed that the reliability index improved by curvatures at the approximate location for the performance function value $\beta_i^{t(k)SORM}$ converges to the component target reliabil-
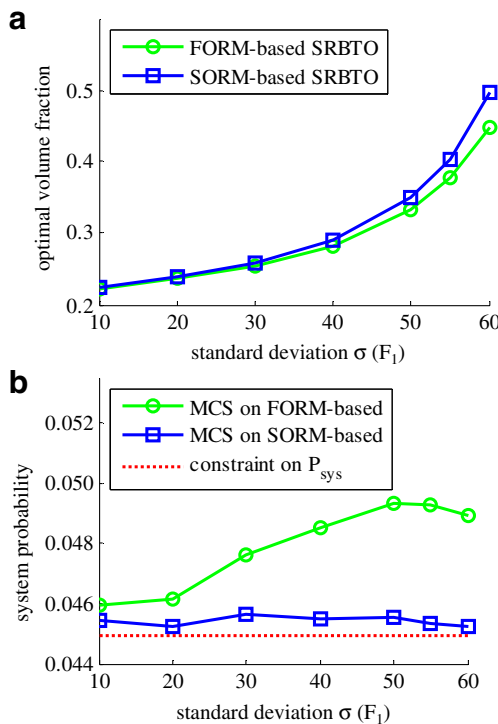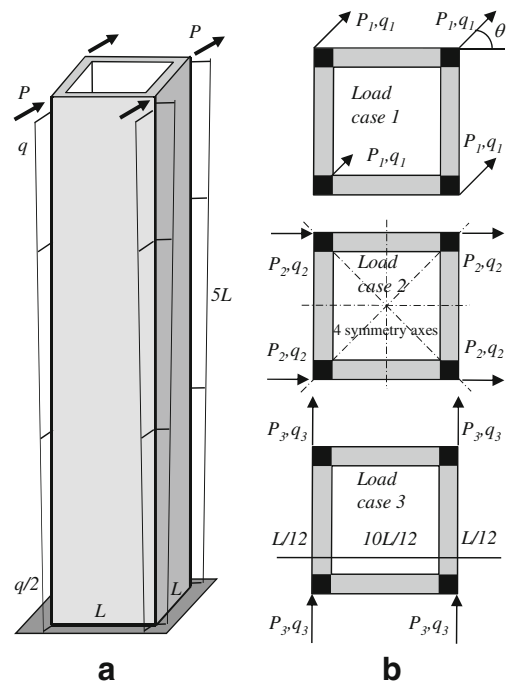

Fig. 12 Building core example: **a** domain of the topology optimization; and **b** load cases

ity index after a few design iterations, which allows for more accurate assessment of the failure probability assessment of the design in achieving the target reliability.

The accuracy of the SORM-based single-loop SRBTO method is also investigated. The FORM-based and SORM-based SRBTO are performed with the system probability target of 0.04493 while standard deviation of load F_1 is varied from 10 to 60. Figure 11a compares the volume fractions by the FORM and SORM-based SRBTOs. It is seen that the FORM-based SRBTO provides unconservative designs due to the inaccuracy in reliability calculations. The results of Monte Carlo simulations (MCS: 10^6 times; c.o.v = 0.005) in Fig. 11b show that the proposed SORM-based SRBTO provides improved accuracy in predicting the system failure probability. In general, the computational cost for the SORM-based approach is more expensive than the FORM-based approach since additional cost is required for calculating the curvatures around the approximate location

Fig. 11 SRBTOs with standard deviation of load F_1: **a** volume fractions of optimal designs; and **b** system failure probabilities

Table 2 Three-dimensional building example: statistical parameters of the load random variables and constraint on the compliances

Load cases	P		q (at top)		C_i^t
	Mean	c.o.v	Mean	c.o.v	
Case 1	70.71	0.30	2.82	0.15	250
Case 2	50.00	0.15	2.00	0.30	125
Case 3	50.00	0.20	2.00	0.15	125

Fig. 13 Building core optimal topologies (three-dimensional and side views): **a** DTO *volfrac* = 21.93%; **b** SRBTO *volfrac* = 28.15% ($P^t_{sys} = 0.05$); and **c** SRBTO *volfrac* = 22.25% ($P^t_{sys} = 0.85$)

a   b   c
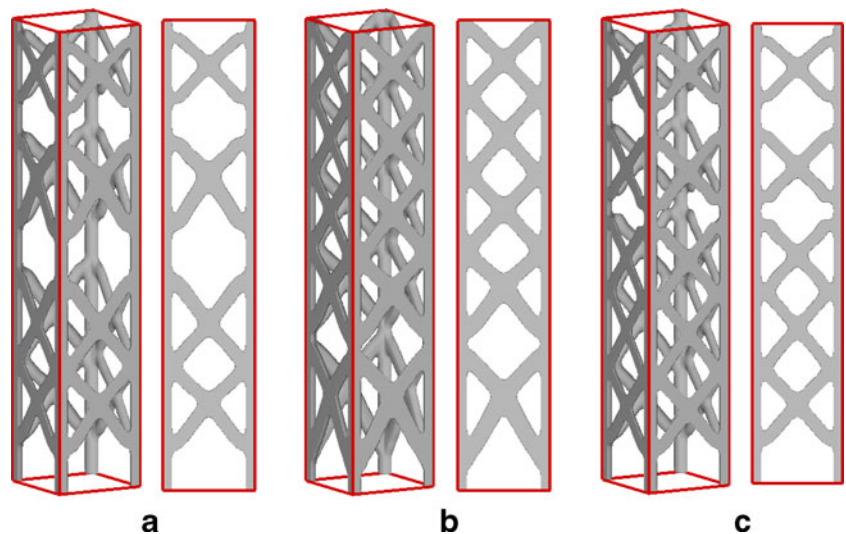
for the performance function value (Breitung 1984; Der Kiureghian 2005); however, the increase of computational time in the numerical examples was moderate while the SORM-based approach allows for significant improvement in accuracy for highly nonlinear reliability problems.

The results in Figs. 10a and 11a show the volume fractions of the optimal designs increase significantly as the load variability increases. It is because the variability of random load increases the uncertainty of the compliance and thus the probability of violating given constraints.

5.3 Three-dimensional building

The proposed SRBTO/MSR method and the MTOP approach allow for system reliability-based optimization for large-scale structural topologies. In this example, the SORM-based SRBTO employing the MTOP approach is applied to design the structural topology of a building core subjected to horizontal loads. The objective of the optimization is to minimize the volume under the constraint on system failure event defined in terms of the compliances for multiple load cases. Figure 12a shows the domain

of the topology with the dimensions of $L \times L \times 5L \times L/12$ in which $L/12$ represents the thickness of the core ($L = 24$). The domain is divided into $12 \times 12 \times 60 \times 1$ B8/n125/d125 MTOP elements, which results in a total of 2,640 brick elements and 330,000 density elements. The four corners of the domain are non-designable regions which are shown as black areas in Fig. 12b. Young's modulus E^0 of 10^6, Poisson's ratio ν of 0.3, the minimum length scale $r_{min} = L/10$, and penalization parameter $p = 4$ are employed. In this example, the building core is designed with four symmetric axes: x, y and two diagonal directions (dash-dot lines in Fig. 12b). We consider three load cases as shown in Fig. 12b. In the first load case, the uncertain point loads (P_1) and the uncertain distributed loads (linearly varying from $q_1/2$ to q_1 along the height as shown in Fig. 12a) are applied with the angle of $\theta = 45°$ (diagonal direction). The second and third load cases have the angle of $\theta = 0°$ (x direction), and $\theta = 90°$ (y direction), respectively. During the finite element analyses, for simplicity, the distributed load is converted to the equivalent point loads applied at the finite element nodes along the height of the building. All six random variables $\{P_1, P_2, P_3, q_1, q_2, q_3\}$ are assumed to

Table 3 Three-dimensional building example: component and system probabilities by SRBTO/MSR and MCS (10^6 times)

			P_1	P_2	P_3	P_{sys}
Case I	$\rho_{same} = 0.50$ $\rho_{diff} = 0.25$	SRBTO/MSR	0.02731	0.02088	0.00539	0.05000
		MCS (c.o.v = 0.005)	0.02747	0.02101	0.00542	0.05023
Case II	$\rho_{same} = 0.50$ $\rho_{diff} = 0.25$	SRBTO/MSR	0.26940	0.25973	0.20818	**0.50000**
		MCS (c.o.v = 0.001)	0.26977	0.26006	0.20800	0.50008
Case III	$\rho_{same} = \textbf{0.90}$ $\rho_{diff} = \textbf{0.45}$	SRBTO/MSR	0.02812	0.02227	0.00625	0.05000
		MCS (c.o.v = 0.004)	0.02816	0.02242	0.00638	0.05017

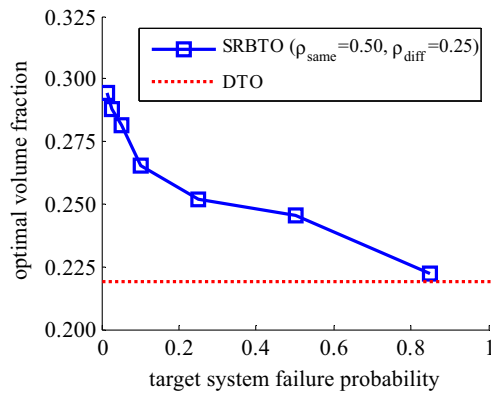The changes from the default case are shown in **bold**

Fig. 14 Optimal volume fractions with target system failure probability

follow normal distributions. Table 2 provides the means and the coefficients of variation (c.o.v) of the random variables and the corresponding constraints given on the compliances of the system. These load random variables are assumed to be correlated with correlation coefficient $\rho_{same} = 0.50$ when they belong to the same load case and the correlation coefficient $\rho_{diff} = 0.25$ for the loads from different load cases.

First of all, the optimization problem is solved without pattern repetition constraints (Case I). The deterministic topology optimization is performed using the mean values of the loads (Fig. 13a) and the SORM-based SRBTO is conducted with the target system probability $P_{sys}^t = 0.05$ on the series system event of compliance limit-states determined for the three load cases (Fig. 13b). The DTO (*volfrac* 21.93%) and SRBTO (*volfrac* 28.15%) resulted in significantly different topologies. The higher volume fraction in the SRBTO topology implies the importance of considering the uncertainties in the loads for building structures. The component and system probabilities of the optimal topologies by SRBTO/MSR and MCS (10^6 times, c.o.v = 0.005) are shown in Table 3, which confirms the accuracy of the SORM-based SRBTO. The component probabilities of 0.02731, 0.02088, and 0.00539 help identify the relative importance ranking of the three constraints as $1 \rightarrow 2 \rightarrow 3$.

Next, we vary the system probability target P_{sys}^t from 0.01 to 0.85 (Case II). Figure 14 shows the volume fractions of the optimal designs for the range. It is seen that the decrease of the target probability (i.e. more conservatism) increases the volume fractions of the optimal designs. The volume fraction of the SRBTO converges to that of DTO as the target probability increases. For example, the target system probability of 0.85 results in the volume fraction of 22.25%, which is only 1.4% different from DTO (21.93%). Even though these two optimal volume fractions are fairly close to each other, it is noteworthy that the optimal topol-

ogy of SRBTO ($P_{sys} = 0.85$) in Fig. 13c is different from that of DTO in Fig. 13a.

The topology optimization problem is solved again using pattern repetition constraints along the vertical direction. This type of pattern repetition constraint is included for both DTO and SRRBTO in this numerical example. The number of pattern repetitions along the vertical direction (denoted by m) is varied from 1 to 12 to investigate the impact of these constraints on the optimal topologies. The optimal topologies by DTO and SRBTO (with $P_{sys}^t = 0.05$) are shown in Fig. 15a and b, respectively. Figure 15 demonstrates significant impacts of the pattern repetition

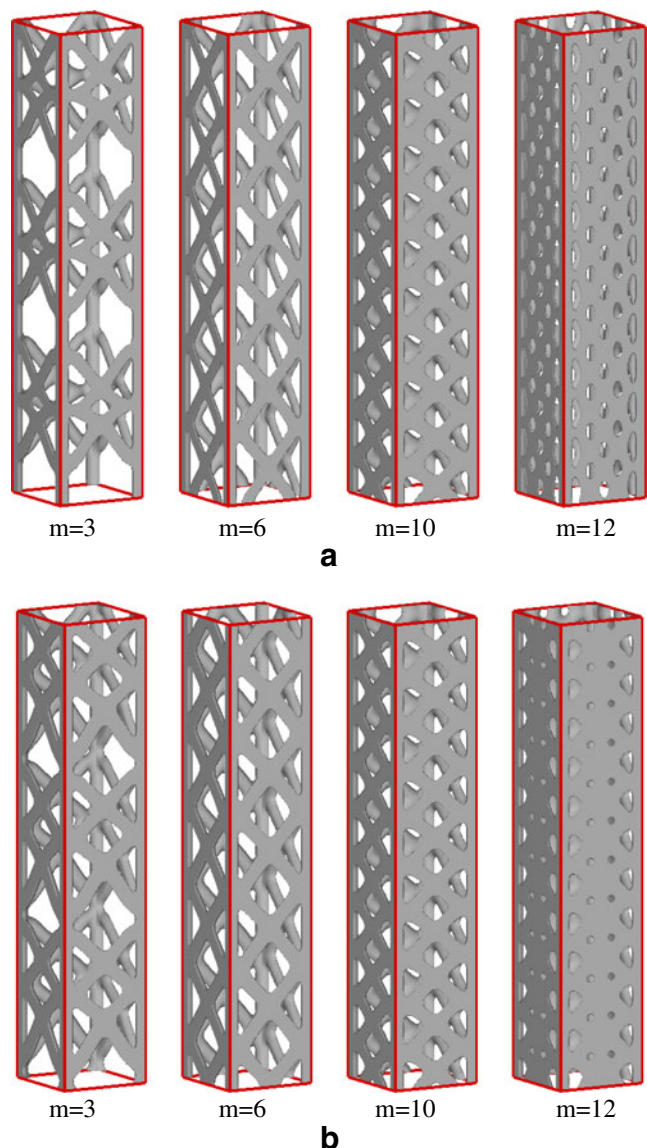**Fig. 15** Building core optimal topologies with pattern repetition: **a** DTO; and **b** SRBTO ($\rho_{same} = 0.50$, $\rho_{diff} = 0.25$, $P_{sys}^t = 0.05$)
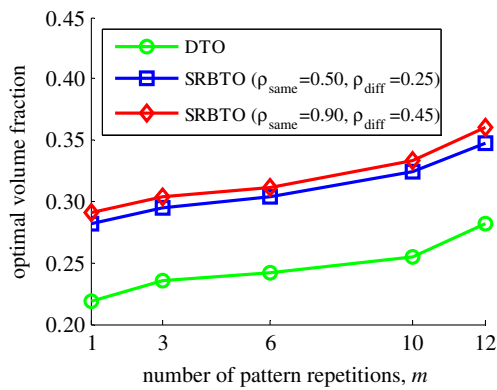
Fig. 16 Optimal volume fraction with the number of pattern repetition ($P_{sys}^t = 0.05$)

constraints on optimal topologies and topologies. The effect of the correlation coefficients is also investigated by increasing the correlation coefficients (Case III). Figure 16 shows the optimal volume fractions versus the number of pattern repetitions, m by DTO, SRBTO ($\rho_{same} = 0.50$, $\rho_{diff} = 0.25$), and SRBTO ($\rho_{same} = 0.90$, $\rho_{diff} = 0.45$). A larger number of patterns results in more constrained optimization problem, and thus provides higher volume fractions. Impacts of the correlation between uncertain loads are also observed.

6 Summary and conclusions

This paper presents three research developments for enhancing the theories and applications of component and system reliability-based topology optimization (CRBTO and SRBTO): (1) developing a single-loop SRBTO approach that employs the matrix-based system reliability (MSR) method to handle the statistical dependence between multiple limit-states; (2) developing SORM-based single-loop approaches for CRBTO and SRBTO to improve the accuracy in evaluating probabilistic constraints; and (3) incorporating multiresolution topology optimization (MTOP) approach to CRBTO and SRBTO in order to obtain high resolution design with a relatively low computation cost with a capability of imposing pattern repetition and symmetric constraints. Three numerical examples of two- and three-dimensional structures demonstrate that (1) uncertainties in TO problems can make significant impact on optimal topologies; (2) if SRBTO problem (i.e. TO with probabilistic constraint given on a system event, not on individual limit-states) is solved by CRBTO approaches, it is hard to determine corresponding component target failure probabilities and the problem becomes more constrained in general; (3) statistical dependence between limit-states can be suc-

cessfully incorporated by use of the MSR method, which may cause a significant difference in optimal topologies; (4) SORM-based RBTO approaches provide optimal designs with improved accuracy in satisfying component and system probabilistic constraints; and (5) MTOP approach enables us to perform CRBTOs and SRBTOs of large-scale TO problems with low computational cost and is capable of imposing pattern symmetry and repetitions in large-scale RBTO problems.

Nomenclature

B	strain-displacement matrix of shape function derivatives
c	"event" vector
d	vector of design variables
D($\cdot$)	constitutive matrix determined by material density function
d_n	the n-th design variable
D^0	constitutive matrix corresponding to the solid material
E_i	the i-th failure event
E_{sys}	the system failure event
E^0	Young's modulus corresponding to the solid material
$f(\cdot)$	objective function
f	global load vector
$g_i(\rho, \mathbf{X})$	limit-state (or performance) function of the i-th failure mode
$g_{P_i^t}$	performance function of the i-th failure mode
$J_{x,u}$	Jacobian matrix of the transformation $\mathbf{x} = \mathbf{x}(\mathbf{u})$
K	global stiffness matrix
K$_e$	element stiffness matrix
p	penalization parameter
p	"probability" vector
P_i	actual failure probability of the i-th mode
P_i^t	target failure probability of the i-th mode
P_{sys}	actual system failure probability
P_{sys}^t	target system failure probability
r_{ik}	Dunnett-Sobel correlation parameter
r_{min}	minimum length scale
r_{ni}	distance from the point associated design variable to the centroid
S	common source random variables
$\mathbf{u}_d$	displacement vector

$\tilde{\mathbf{u}}_i^t$	approximate location for the performance function value for the i-th failure mode
$\tilde{\mathbf{u}}_i$	approximate location for the performance function value by the KKT condition
volfrac	volume fraction
V_s	prescribed volume constraint
$\mathbf{X}$	random variables
$\hat{\boldsymbol{\alpha}}_i$	negative normalized gradient vector
β_i	reliability index
β_i^t	target reliability index
$\beta_i^{t(k)}$	updated target reliability index at the k-th design iteration
$\beta_i^{t(k)(SORM)}$	improved reliability index using Breitung's formula at the k-th design iteration
$\boldsymbol{\mu_x}$	vector of means of x
$\rho(\cdot)$	material density function
ρ_i	density of element i
$\boldsymbol{\psi}$	position vector

References

Allen M, Raulli M, Maute K, Frangopol DM (2004) Reliability-based analysis and design optimization of electrostatically actuated MEMS. Comput Struct 82(13–14):1007–1020

Almeida SRM, Paulino GH, Silva ECN (2010) Material gradation and layout in topology optimization of functionally graded structures: a global–local approach. Struct Multidiscipl Optim 42(6):855–868

Amir O, Bendsoe MP, Sigmund O (2009) Approximate reanalysis in topology optimization. Int J Numer Methods Eng 78(12):1474–1491

Amir O, Stolpe M, Sigmund O (2010) Efficient use of iterative solvers in nested topology optimization. Struct Multidiscipl Optim 42(1):55–72

Bae K, Wang S, Choi KK (2002) Reliability-based topology optimization. In: AIAA 2002-5542, 9th AIAA/ISSMO symposium on multidisciplinary analysis and optimization, 4–6 September 2002, Atlanta, USA

Bendsøe MP (1989) Optimal shape design as a material distribution problem. Struct Multidiscipl Optim 1(4):193–202

Bendsøe MP, Sigmund O (2003) Topology optimization: theory, methods, and applications. Springer, Berlin

Bjerager P, Krenk S (1989) Parametric sensitivity in first order reliability theory. J Eng Mech 115(7):1577–1582

Borrvall T, Petersson J (2001) Large-scale topology optimization in 3D using parallel computing. Comput Methods Appl Mech Eng 190(46–47):6201–6229

Breitung K (1984) Asymptotic approximations for multinormal integrals. J Eng Mech 110:357–366

Chen S, Chen W, Lee S (2010) Level set based robust shape and topology optimization under random field uncertainties. Struct Multidiscipl Optim 41(4):507–524

Der Kiureghian A (2005) First-and second-order reliability methods. Engineering design reliability handbook, Ch 14. CRC, Boca Raton, Florida

Du XP, Chen W (2004) Sequential optimization and reliability assessment method for efficient probabilistic design. J Mech Des 126(2):225–233

Dunnett CW, Sobel M (1955) Approximations to the probability integral and certain percentage points of a multivariate analogue of student's t-distribution. Biometrika 42(1–2):258–260

Enevoldsen I, Sørensen JD (1994) Reliability-based optimization in structural engineering. Struct Saf 15(3):169–196

Eschenauer HA, Olhoff N (2001) Topology optimization of continuum structures: a review. Appl Mech Rev 54(4):331–389

Evgrafov A, Rupp CJ, Maute K, Dunn ML (2008) Large-scale parallel topology optimization using a dual-primal substructuring solver. Struct Multidiscipl Optim 36(4):329–345

Guest JK, Igusa T (2008) Structural optimization under uncertain loads and nodal locations. Comput Methods Appl Mech Eng 198(1):116–124

Guest JK, Prévost JH, Belytschko T (2004) Achieving minimum length scale in topology optimization using nodal design variables and projection functions. Int J Numer Methods Eng 61(2):238–254

Jung HS, Cho S (2004) Reliability-based topology optimization of geometrically nonlinear structures with loading and material uncertainties. Finite Elem Anal Des 41(3):311–331

Kang J, Kim C, Wang S (2004) Reliability-based topology optimization for electromagnetic systems. Compel Int J Comput Math Elect Electr Eng 23(3):715–723

Kang W-H, Song J, Gardoni P (2008) Matrix-based system reliability method and applications to bridge networks. Reliab Eng Syst Saf 93:1584–1593

Kang W-H, Lee Y-J, Song J, Gencturk B (2011) Further development of matrix-based system reliability method and applications to structural systems. Struct Infrastruct Eng, in print. doi:10.1080/15732479.2010.539060

Kharmanda G, Olhoff N, Mohamed A, Lemaire M (2004) Reliability-based topology optimization. Struct Multidiscipl Optim 26(5):295–307

Kim C, Wang S, Rae K, Moon H, Choi KK (2006) Reliability-based topology optimization with uncertainties. J Mech Sci Technol 20(4):494–504

Lee I, Choi KK, Gorsich D (2010) System reliability-based design optimization using the MPP-based dimension reduction method. Struct Multidiscipl Optim 41(6):823–839

Lee Y-J, Song J, Gardoni P, Lim H-W (2011) Post-hazard flow capacity of bridge transportation network considering structural deterioration of bridges. Struct Infrastruct Eng 7(7):509–521

Liang J, Mourelatos ZP, Nikolaidis E (2007) A single-loop approach for system reliability-based design optimization. J Mech Des 129(12):1215–1224

Liang J, Mourelatos ZP, Tu J (2008) A single-loop method for reliability-based design optimisation. Int J Prod Dev 5(1–2):76–92

Lógó J, Ghaemi M, Rad MM (2009) Optimal topologies in case of probabilistic loading: the influence of load correlation. Mech Based Des Struct Mach 37(3):327–348

Luo Y, Kang Z, Luo Z, Li A (2009) Continuum topology optimization with non-probabilistic reliability constraints based on multiellipsoid convex model. Struct Multidiscipl Optim 39(3):297–310

Maute K, Frangopol DM (2003) Reliability-based design of MEMS mechanisms by topology optimization. Comput Struct 81(8–11):813–824

McDonald M, Mahadevan S (2008) Design optimization with system-level reliability constraints. J Mech Des 130(2):021403-1-10

Mogami K, Nishiwaki S, Izui K, Yoshimura M, Kogiso N (2006) Reliability-based structural optimization of frame structures for multiple failure criteria using topology optimization techniques. Struct Multidiscipl Optim 32(4):299–311

Nguyen TH (2010) System reliability-based design and multiresolution topology optimization. PhD thesis, Department of Civil and Environmental Engineering, University of Illinois at Urbana-Champaign

Nguyen TH, Paulino GH, Song J, Le CH (2010a) A computational paradigm for multiresolution topology optimization (MTOP). Struct Multidiscipl Optim 41(4):525–539

Nguyen TH, Song J, Paulino GH (2010b) Single-loop system reliability-based design optimization using matrix-based system reliability method: theory and applications. J Mech Des 132(1):011005-1-11

Rahman S, Wei D (2008) Design sensitivity and reliability-based structural optimization by univariate decomposition. Struct Multidiscipl Optim 35(3):245–261

Royset JO, Der Kiureghian A, Polak E (2001) Reliability-based optimal structural design by the decoupling approach. Reliab Eng Syst Saf 73(3):213–221

Royset JO, Der Kiureghian A, Polak E (2006) Optimal design with probabilistic objective and constraints. J Eng Mech 132(1):107–118

Rozvany GIN (2001) Aims, scope, methods, history and unified terminology of computer-aided topology optimization in structural mechanics. Struct Multidiscipl Optim 21(2):90–108

Rozvany GIN (2008) Exact analytical solutions for benchmark problems in probabilistic topology optimization. In: EngOpt 2008–international conference on engineering optimization, Rio de Janeiro

Rozvany GIN, Zhou M, Birker T (1992) Generalized shape optimization without homogenization. Struct Multidiscipl Optim 4(3):250—252

Shan S, Wang GG (2008) Reliable design space and complete single-loop reliability-based design optimization. Reliab Eng Syst Saf 93(8):1218–1230

Silva M, Tortorelli DA, Norato JA, Ha C, Bae HR (2010) Component and system reliability-based topology optimization using a single-loop method. Struct Multidiscipl Optim 41(1):87–106

Song J, Kang W-H (2009) System reliability and sensitivity under statistical dependence by matrix-based system reliability method. Struct Saf 31(2):148–156

Song J, Ok S-Y (2010) Multi-scale system reliability analysis of lifeline networks under earthquake hazards. Earthquake Eng Struct Dyn 39(3):259–279

Sutradhar A, Paulino GH, Miller MJ, Nguyen TH (2010) Topological optimization for designing patient-specific large craniofacial segmental bone replacements. Proc Nat Acad Sci USA 107(30):13222–13227

Svanberg K (1987) The method of moving asymptotes—a new method for structural optimization. Int J Numer Methods Eng 24(2):359–373

Tu J, Choi KK, Park YH (1999) A new study on reliability-based design optimization. J Mech Des 121(4):557–564

Wang S, de Sturler E, Paulino GH (2007) Large-scale topology optimization using preconditioned Krylov subspace methods with recycling. Int J Numer Methods Eng 69(12):2441–2468

Wu YT, Wang W (1998) Efficient probabilistic design by converting reliability constraints to approximately equivalent deterministic constraints. J Integr Des Process Sci 2(4):13–21

Xu H, Rahman S (2005) Decomposition methods for structural reliability analysis. Probab Eng Mech 20(3):239–250

Yang RJ, Chuang C, Gu L, Li G (2005) Experience with approximate reliability-based optimization methods II: an exhaust system problem. Struct Multidiscipl Optim 29(6):488–497